

Clinical Impact of Size, Shape, and Orientation of the Tricuspid Annulus in Tricuspid Regurgitation as Assessed by Three-Dimensional Echocardiography

Hiroto Utsunomiya, MD, Yuji Itabashi, MD, Sayuki Kobayashi, MD, Florian Rader, MD, Robert J. Siegel, MD, FASE, and Takahiro Shiota, MD, FASE, *Los Angeles, California*

Background: Tricuspid annuloplasty for tricuspid regurgitation (TR) depends on the measurements of tricuspid annular diameter (TAD) obtained in an apical four-chamber view on two-dimensional (2D) transthoracic echocardiography (TTE). We performed a combined 2D and three-dimensional (3D) echocardiographic study to understand the impact of the size, shape, and orientation of a dilated annulus on the inconsistencies between measured 2D TTE-TAD and the actual annular diameter.

Methods: A total of 185 patients with grade $\geq 3+$ TR and 50 controls underwent 2D TTE and 3D transesophageal echocardiography (TEE) assessment of the tricuspid valve. The 3D TEE-TAD, defined as the longest dimension, and tricuspid annulus (TA) eccentricity index, defined as the shortest/longest dimension ratio, were obtained. The angle between the major tricuspid annulus axis and interatrial septum parallel to the vertical axis (α°) was measured as an index of TA orientation.

Results: Compared with controls, TR subgroups had a larger α° irrespective of TR etiology and cardiac rhythm ($P < .05$), with the posteriorly displaced TA most frequently noted in patients with atrial fibrillation. An excellent correlation was found between 3D TEE-TAD and 2D TTE-TAD, but 2D TTE-TAD was significantly smaller than 3D TEE-TAD (35.9 ± 5.4 vs 39.8 ± 5.7 mm; $P < .001$; bias, 3.9 ± 2.6 mm; limits of agreement, -1.1 - 8.9 mm). After multivariate adjustment, a larger 3D TEE-TAD and larger absolute value of $90^\circ - \alpha^\circ$ were independent determinants of the bias between 3D TEE-TAD and 2D TTE-TAD (both $P < .001$).

Conclusions: The inconsistencies between measured 2D TTE-TAD and the actual annular diameter can be explained through morphologic factors such as TA size and orientation. (J Am Soc Echocardiogr 2019; ■: ■-■.)

Keywords: 3D echocardiography, Transesophageal echocardiography, Transthoracic echocardiography, Tricuspid annular diameter, Valvular heart disease

Tricuspid regurgitation (TR) is a relatively common valvular heart disease in clinical practice¹ and, when severe, is associated with increased mortality regardless of pulmonary hypertension and left ventricular systolic function.² Concomitant tricuspid valve (TV) annu-

loplasty is recommended at the time of left-sided valve surgery because of its beneficial effect on right ventricular (RV) function and remodeling,³ but the surgical decision-making depends heavily on the measurements of tricuspid annulus (TA) size. Conventional two-dimensional (2D) transthoracic echocardiography (TTE) is a widely accepted diagnostic tool for the assessment of TA size; therefore, current guidelines recommend that TA diameter (TAD) measurements be made in an apical four-chamber view on 2D TTE.^{4,5} However, 2D TTE-TAD and its thresholds for TA enlargement are not well validated. Furthermore, TA geometry has been shown to have a complex three-dimensional (3D) shape.⁶ As surgical tricuspid annuloplasty and new percutaneous tricuspid devices are improving over time, more accurate sizing of the TA and detailed interpretation of 2D TTE-TAD are required.

Recently introduced 3D echocardiography can provide more accurate geometric information on the TV, whereas 2D TTE-based TV assessment may be limited by the angle and location of the 2D plane.^{7,8} Notably, real-time 3D transesophageal echocardiography (TEE) studies suggested various shapes and orientations of the dilated TA in association with TR severity and etiology.^{9,10} These findings evoke the hypothesis that currently performed 2D measurements

From the Smidt Heart Institute, Cedars-Sinai Medical Center, Los Angeles, California.

This work was partially supported by Merck Sharp and Dohme (MSD) Life Science Foundation, Public Interest Incorporated Foundation. This work was also supported by Takeda Science Foundation and Japan Society for the Promotion of Science Grants-in-Aid for Scientific Research (grant no. JP17K16008).

Conflicts of Interest: Drs. Siegel and Shiota are speakers for Philips Ultrasound. All other authors have reported they have no relationships relevant to the contents of this paper to disclose.

Reprint requests: Takahiro Shiota, MD, FASE, Smidt Heart Institute, Cedars-Sinai Medical Center, 127 South San Vicente Boulevard, A3411, Los Angeles, California (E-mail: ShiotaT@cshs.org).

0894-7317/\$36.00

Copyright 2019 by the American Society of Echocardiography.

<https://doi.org/10.1016/j.echo.2019.09.016>

Abbreviations

2D = Two-dimensional
3D = Three-dimensional
3DQ = Three-dimensional quantification
AF = Atrial fibrillation
ANOVA = Analysis of variance
MVN = Mitral valve navigator
RA = Right atrial
RV = Right ventricular, ventricle
SR = Sinus rhythm
TA = Tricuspid annulus
TAD = Tricuspid annular diameter
TEE = Transesophageal echocardiography
TR = Tricuspid regurgitation
TTE = Transthoracic echocardiography
TV = Tricuspid valve

and the diagnostic accuracy of 2D TTE-TAD for TA enlargement using recommended thresholds (≥ 40 mm or 21 mm/m²) would be affected by TA shape and orientation, highlighting the need for reappraising the methodology for the measurement of TAD.

Therefore, the purposes of the present study were to characterize TA deformations using 3D TEE in patients with grade $\geq 3+$ TR with various underlying etiologies and to investigate the diagnostic accuracy of 2D TTE-TAD for TA dilatation using 3D TEE-derived TAD as the reference standard.

METHODS**Patient Population**

This is a cross-sectional, observational study of 185 patients with grade $\geq 3+$ TR with various underlying causes including primary TR and functional TR, retrospectively recruited from

January 2014 to December 2015 as part of a large 3D TV cohort study whose aim was to provide comprehensive data for quantitative parameters obtained with 3D TEE.¹⁰ All patients underwent 2D TTE and 3D TEE assessment of the TV on the same day. The protocol of this study was approved by the Cedars-Sinai Institutional Review Board. Additionally, measurements of 2D and 3D TV parameters were obtained from 50 normal controls who were referred to the echocardiography laboratory to investigate the cause of transient ischemic attack or atypical chest pain. TR or heart failure was ruled out by a health questionnaire, physical examination, and echocardiography. No controls had any echocardiographic abnormality including TV or right-sided chambers and thus could be considered as having normal TV geometry.

Two-Dimensional TTE

A comprehensive 2D TTE with a focus in the TV and the right ventricle (RV) was performed using a commercially available ultrasound system (S5-1 probe; IE33, Philips, Andover, MA). Using the zoom mode focused on the TV, images were acquired in an apical four-chamber view. Measurements of the 2D TTE-TAD were performed off-line by the first author and the echocardiography specialist (level III trained) in mid-diastole at the time of the maximum TV opening between the two hinge points at the junction between the TV leaflets and the TA (Figure 1). In patients with atrial fibrillation (AF), three to five cycles were analyzed and averaged to determine the value of 2D TTE-TAD. The RV was imaged from multiple views, including an RV-focused apical four-chamber view. Two-dimensional right-sided chamber size and function were measured according to the American Society of Echocardiography guidelines for the echocardi-

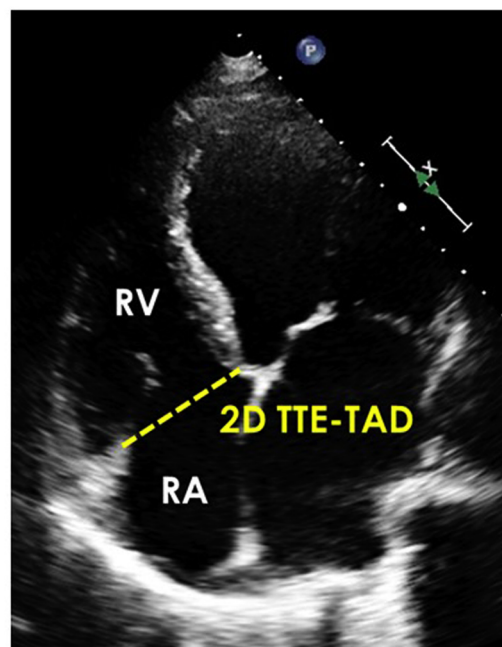


Figure 1 Measurements of 2D TTE-TAD were performed in the apical four-chamber view in mid-diastole at the time of the maximum TV opening between the two hinge points at the junction between the leaflets and the annulus (yellow dotted line). RA, Right atrium.

graphic assessment of the right heart.⁴ Right atrial (RA) volume was calculated using single-plane disk summation techniques in a dedicated apical four-chamber view. Systolic pulmonary artery pressure was calculated from the systolic RV pressure gradient and RA pressure. RA pressure was estimated from the inferior vena cava diameter and respiratory changes.⁴ Grading TR severity was determined by using a multiparametric integrated approach.¹¹ The vena contracta width was also measured from the apical four-chamber and parasternal RV inflow views during held end expiration. Average vena contracta width from these two roughly orthogonal views was calculated to account for its noncircular and ellipsoidal shape.¹²

Three-Dimensional TEE

Three-dimensional TEE was performed under sedation using intravenous injection of midazolam using an IE33 or EPIQ7 ultrasound imaging system equipped with a fully sampled matrix-array TEE transducer (X7-2t Live 3D TEE transducer, Philips), which can display both 2D and 3D images. At first, the 2D TV images were clearly demonstrated in the midesophageal oblique short-axis view, coronary sinus view, or transgastric RV inflow view (Figure 2A). Then volume data sets were obtained using the live 3D zoom mode ($n = 80$; median frame rate = 14 Hz) or six-beat full-volume mode ($n = 105$; median frame rate = 40 Hz) focused on the TV (Figure 2B, left panel). In patients with AF, the live 3D zoom mode with one-beat volume acquisition was chosen to avoid stitch artifacts. The view was optimized for depth and gain setting before 3D acquisition, and close attention was given to including the entire TV and RV in the sector boundaries. All 3D TEE data were digitally stored for off-line analysis, and TomTec's 4D RV Function (TomTec, Munich, Germany) was used to measure RV volumes.

HIGHLIGHTS

- Patients with TR have a more dilated, circular, and posteriorly displaced TA.
- AF rhythm, rather than TR etiology, is related to more posteriorly TA expansion.
- TA orientation is a crucial determinant of the underestimation of 2D TTE-TAD.

TR Subgroup Determination

Before 3D TA quantitative analysis, the initial 3D TV screening was performed to reveal an anatomic abnormality in the TV leaflets and to determine TR etiology.¹⁰ For the initial TV screening, the live 3D zoom or full-volume data set was imported into the QLAB 3D quantification (3DQ) software package (Philips). The 2-orthogonal long-axis planes through the TV were reconstructed. These planes roughly corresponded to the RV-focused apical four-chamber and the parasternal RV inflow views on 2D TTE. On the short-axis plane, the 2-orthogonal long-axis planes are shifted throughout the TV to determine primary TR with the presence of organic TV

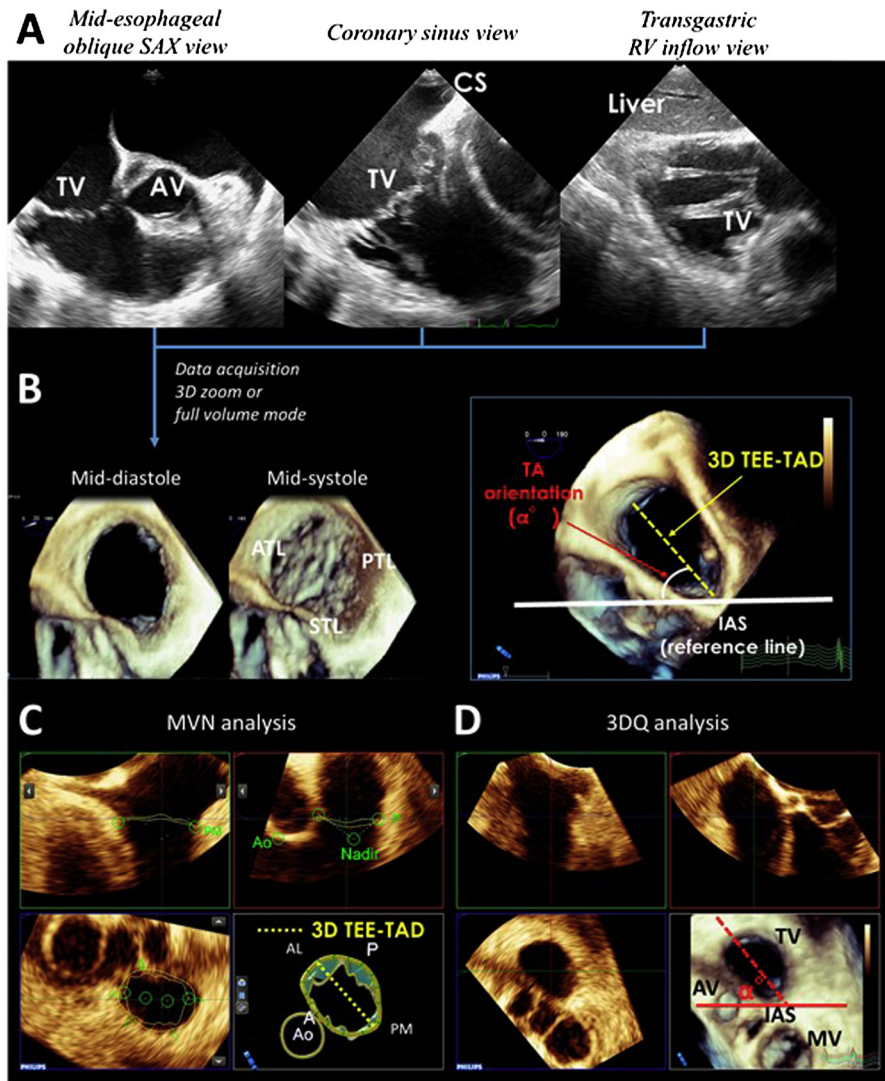


Figure 2 Three-dimensional TEE data acquisition and analysis. **(A)** 2D TEE: TV images were clearly demonstrated in the mid-esophageal oblique short-axis view, coronary sinus view, or transgastric RV inflow view. **(B)** 3D volume rendering: volume data sets were obtained using the live 3D zoom mode or six-beat full-volume mode to view the TV from the RA perspective in mid-diastole and midsystole (left panel). To grasp the whole picture of the TV for TA orientation, 3D volume rendering was first interrogated and displayed with the interatrial septum placed inferiorly in the 6 o'clock position (right panel). **(C)** MVN: Anteroposterior (A-P) and anterolateral-posteromedial (AL-PM) directions were determined based on the commissure between anterior and septal leaflets as an anterior direction. The 3D TEE-TAD, defined as the longest dimension; TA area; height; and TA eccentricity index, defined as the shortest/longest dimension ratio, were obtained on the mid-diastolic frame. **(D)** 3DQ: the TV can be displayed using three orthogonally oriented planes in mid-diastole at the time of the maximum valve opening. The short-axis image of the TV was generated carefully using guidance on the corresponding 3D TV image, in which the aortic valve (Ao) is located on the left, the mitral valve on the bottom, and the TV on the top. The angle between the major TA axis and interatrial septum parallel to the vertical axis (α°) was measured as an index of TA orientation. A, Anterior; ATL, anterior tricuspid leaflet; AV, aortic valve; CS, coronary sinus; IAS, interatrial septum; MV, mitral valve; PTL, posterior tricuspid leaflet; SAX, short axis; STL, septal tricuspid leaflet.

disease. After the 3D TV screening, the functional TR group was categorized as one of the following four types through an in-depth chart review: (1) functional TR because of left-sided heart disease including valve disease or left ventricular dysfunction; (2) functional TR resulting from any causes of pulmonary arterial hypertension; (3) functional TR resulting from any cause of RV dysfunction; (4) functional TR secondary to chronic AF.¹⁰ Because of the multiplicity and complexity of causes of TR, study population subgroups were simply stratified by etiology (functional vs primary) and cardiac rhythm (AF vs sinus rhythm [SR]) for the comparison of size, shape, and orientation of the TA.

TA Quantitative Analysis

TA Size and Shape. The live 3D zoom or full-volume data set was imported into the workstation (QLAB ver. 10.7; Philips). The mitral module of the QLAB mitral valve navigator (MVN) software (Philips) was used in an off-label fashion for semiautomated indirect measurement of 3D TEE-TAD during diastole. As previously described in our study,¹⁰ we used 20 landmarks to delineate the TA and analyzed the TV leaflets using ≤ 22 intersections per patient. Anteroposterior and anterolateral-posteromedial directions were determined based on the commissure between anterior and septal leaflets as an anterior direction. The 3D TEE-TAD, defined as the longest dimension (Figure 2C); TA area; height; and TA eccentricity index, defined as the shortest/longest dimension ratio, were obtained on the mid-diastolic frame. In patients with AF, three measurements from three different beats were averaged.

TA Orientation. To grasp the whole picture of the TV for TA orientation, 3D volume rendering was first interrogated and displayed with the interatrial septum placed inferiorly in the 6 o'clock position (Figure 2B, right panel).¹³ Using the 3DQ software, the TV can be displayed using three orthogonally oriented planes in mid-diastole at the time of the maximum valve opening. The short-axis image of the TV was generated carefully using guidance on the corresponding 3D TV image, in which the aortic valve is located on the left, the mitral valve on the bottom, and the TV on the top. Then the angle between the major TA axis and interatrial septum parallel to the vertical axis (α°) was directly measured as an index of TA orientation (Figure 2D). This angle represents the direction of TA expansion. The remaining 2-orthogonal long-axis planes approximately corresponded to the RV-focused apical four-chamber and the parasternal RV inflow views.

Substudy Analysis for the TTE-TAD Measured with Both 2D and 3D Echocardiography

In a subset of 46 patients with TR (10 primary TR and 36 functional TR), 3D TTE volume data sets were also obtained using the live 3D zoom mode ($n = 16$; median frame rate = 10 Hz) or four-beat full-volume mode ($n = 30$; median frame rate = 29 Hz) focused on the TV. Using the QLAB MVN software, semiautomated indirect measurement of 3D TTE-TAD was performed and compared with 3D TEE-TAD and 2D TTE-TAD. Annular measurements were performed at mid-diastole, defined as the frame at the time of the maximum TV opening. The 3D TTE-TAD was defined as the longest dimension of the annulus.

Statistical Analysis

Continuous variables are expressed as mean \pm SD. Group comparisons were performed by one-way analysis of variance (ANOVA) with post hoc test using the Tukey's test or the Steel-Dwass method for variables with or without normal distribution, respectively. Correlations

of the TA orientation with the RA and RV volumes were assessed using Pearson's correlation coefficient and linear regression. To identify determinants of the bias between 3D TEE-TAD and 2D TTE-TAD, linear regression was performed for multivariate analysis. The covariates were chosen as demographic variables and 3D TA parameters including 3D TEE-TAD, TA eccentricity index, and the absolute value of $90^\circ - \alpha^\circ$. These three parameters represent TA size, shape, and orientation, respectively. The 2D TTE-TAD was compared with the 3D TEE-TAD using a paired *t* test and Pearson's correlation coefficient. The accuracy of 2D TTE-TAD was tested using Bland-Altman analysis as compared with 3D TEE-TAD.

Reproducibility of 3D TEE-TAD measurements, as described by absolute difference \pm SD and intraclass correlations, was evaluated in 20 TV data sets a month after the initial measurement by first author for intraobserver variability and by a second observer for interobserver variability. The second observer selected the same TV data set and the frame that the first observer used and performed 3D analysis independently. All analyses were performed using SPSS version 21.0 (IBM, Armonk, NY).

RESULTS

TR Subgroups

The study population comprised 85 men and 100 women with a mean age of 70 ± 15 years. The severity of TR was 3+ in 111 patients and 4+ in 74 patients, with a mean vena contracta width of 5.9 ± 1.6 mm. The cardiac rhythm at the time of the TEE procedure was AF in 80 patients (43.2%) and SR in 105 (56.8%). Seventeen patients (9.2%) had pacemaker or implantable cardioverter-defibrillator lead. Among 185 TR patients, the initial 3D TV screening revealed an anatomical abnormality in the TV leaflets of 38 patients (20.5%) including 12 lead-associated TRs, 10 rheumatic heart diseases, eight myxomatous degenerations, five cases of endocarditis, and one carcinoid disease. After the 3D TV screening, 147 (79.5%) patients were categorized as having functional TR with structurally normal TV leaflets. The breakdown of functional TR was as follows: left-sided heart disease-TR, $n = 106$; pulmonary arterial hypertension-TR, $n = 4$; RV dysfunction-TR, $n = 1$; AF-TR, $n = 36$.

Clinical and Echocardiographic Parameters

The clinical and echocardiographic parameters of the normal controls and patients with TR subgroups are listed in Table 1. Comparison of functional versus primary TR showed that functional TR was associated with a higher systolic pulmonary artery pressure and a larger RV end-systolic volume with worse biventricular function (all $P < .05$ after multiple comparisons; Table 1). On the other hand, comparison of the AF group versus the SR group showed that patients with AF were associated with a lower systolic pulmonary artery pressure and a smaller RV end-systolic volume and larger RA volume with preserved biventricular function, resulting in a higher RA/RV end-systolic volume ratio (all $P < .05$ after multiple comparisons; Table 1).

TV Parameters

The TV parameters of the normal controls and patients with TR subgroups are shown in Table 2. Compared with the normal controls, TR patients showed a 22% increase in the 3D TEE-TAD (33.9 ± 1.8 vs 41.4 ± 5.3 mm; $P < .001$), a 70% increase in the TA area in mid-diastole (754 ± 83 vs $1,281 \pm 338$ mm²; $P < .001$), a 21% increase

Table 1 Clinical and echocardiographic parameters of normal controls and patients according to TR subgroups

	Etiology			P (ANOVA)	Cardiac rhythm		P (ANOVA)
	Normal TV (n = 50)	Functional (n = 147)	Primary (n = 38)		AF (n = 80)	SR (n = 105)	
Age, y	60 ± 11	72 ± 14 ^{*†}	64 ± 15	<.001	74 ± 11 ^{*‡}	67 ± 16 [*]	<.001
Sex, female	23 (46.0)	71 (48.3) [†]	28 (73.7) [*]	.013	47 (58.8)	52 (49.5)	.29
Body surface area, m ²	1.8 ± 0.2	1.9 ± 0.3	1.8 ± 0.2	.09	1.8 ± 0.3	1.9 ± 0.2	.87
AF	0 (0)	63 (42.9) [*]	17 (44.7) [*]	<.001	80 (100)	0 (0)	<.001
Average vena contracta width, mm	N/A	5.9 ± 1.5	6.3 ± 1.6	.15	5.9 ± 1.4	5.9 ± 1.6	.92
Systolic pulmonary artery pressure, mm Hg	22.8 ± 6.5	55.8 ± 16.7 ^{*†}	40.5 ± 11.5 [*]	<.001	46.2 ± 13.7 ^{*‡}	59.1 ± 16.2 [*]	<.001
RV end-diastolic volume, mL	70 ± 18	120 ± 53 [*]	110 ± 48 [*]	<.001	102 ± 43 ^{*‡}	131 ± 54 [*]	<.001
RV end-systolic volume, mL	33 ± 10	76 ± 44 ^{*†}	62 ± 33 [*]	<.001	57 ± 34 ^{*‡}	86 ± 43 [*]	<.001
RV ejection fraction, %	51 ± 5	39 ± 12 ^{*†}	47 ± 7	<.001	46 ± 10 ^{*‡}	36 ± 10 [*]	<.001
LV ejection fraction, %	62.2 ± 3.3	52.2 ± 17.2 ^{*†}	61.6 ± 10.1	<.001	58.1 ± 10.8 [‡]	51.1 ± 19.2 [*]	.002
LA volume index, mL/m ²	18.5 ± 1.3	53.8 ± 23.2 [*]	54.6 ± 33.0 [*]	<.001	57.3 ± 29.5 [*]	51.4 ± 21.5 [*]	<.001
RA volume index, mL/m ²	15.8 ± 2.2	49.7 ± 25.6 [*]	46.7 ± 24.5 [*]	<.001	56.1 ± 28.0 ^{*‡}	43.7 ± 21.8 [*]	<.001
RA/RV end-systolic volume ratio	0.8 ± 0.2	1.5 ± 1.1	1.6 ± 1.0	.32	2.1 ± 1.2 ^{*‡}	1.1 ± 0.7 [*]	<.001

Data are expressed as mean ± SD or n (%). LA, Left atrial; LV, left ventricular.

*P < .05 vs normal TV.

†P < .05 vs primary TR.

‡P < .05 vs SR.

Table 2 TV parameters of normal controls and patients according to TR subgroups

	Etiology			P (ANOVA)	Cardiac rhythm		P (ANOVA)
	Normal TV (n = 50)	Functional (n = 147)	Primary (n = 38)		AF (n = 80)	SR (n = 105)	
2D TTE-TAD, mm	30.8 ± 2.3	37.6 ± 5.0 [*]	36.0 ± 5.4 [*]	<.001	37.9 ± 4.6 [*]	36.7 ± 5.5 [*]	<.001
3D TEE-TAD, mm	33.9 ± 1.8	41.9 ± 5.3 ^{*†}	39.5 ± 5.2 [*]	<.001	41.8 ± 5.2 [*]	41.1 ± 5.4 [*]	<.001
Bias between 3D TEE-TAD and 2D TTE-TAD, mm	3.06 ± 1.69	4.29 ± 2.71 [*]	3.57 ± 2.62	.001	3.92 ± 2.75 [*]	4.31 ± 2.66 [*]	.002
TA eccentricity index	0.75 ± 0.05	0.91 ± 0.06 [*]	0.91 ± 0.05 [*]	<.001	0.92 ± 0.05 ^{*‡}	0.90 ± 0.06 [*]	<.001
α°	46.3 ± 9.8	75.9 ± 34.9 [*]	81.4 ± 36.1 [*]	<.001	88.3 ± 36.1 ^{*‡}	68.5 ± 31.9 [*]	<.001
Tenting volume, mL	0.7 ± 0.2	2.7 ± 1.8 ^{*†}	2.0 ± 1.7 [*]	<.001	1.8 ± 1.5 ^{*‡}	3.2 ± 1.8 [*]	<.001

Data are expressed as mean ± SD or n (%).

*P < .05 vs normal TV.

†P < .05 vs primary TR.

‡P < .05 vs SR.

in the TA eccentricity index (0.75 ± 0.05 vs 0.91 ± 0.06 ; $P < .001$), and a 66% increase in the α° ($46.3^\circ \pm 9.8^\circ$ vs $77.0^\circ \pm 35.1^\circ$; $P < .001$). Functional TR had a larger 3D TEE-TAD and tenting volume compared with primary TR (both $P < .05$ after multiple comparison), whereas 2D TTE-TAD, TA eccentricity index, and α° were similar between the TR subgroups. On the other hand, patients with AF showed a higher TA eccentricity index and a larger α° with a smaller tenting volume (all $P < .05$ after multiple comparison), whereas 2D TTE-TAD and 3D TEE-TAD were similar between the TR subgroups.

Distribution of TA Orientation

Distributions of TA orientation in the total patient population and according to TR subgroups are shown in Figure 3.

Notably, the two most frequent orientations were demonstrated in the histogram (Figure 3A). Compared with patients with normal TV, TR subgroups had a larger α° irrespective of TR etiology and cardiac rhythm (all $P < .05$; Table 2). In particular, the TR subgroup with AF had a larger α° than the normal TV group and the TR subgroup with SR ($88.3^\circ \pm 36.1^\circ$ vs $46.3^\circ \pm 9.8^\circ$ vs $68.5^\circ \pm 31.9^\circ$, $P < .05$ after multiple comparisons; Table 2). The posteriorly displaced TA ($\alpha^\circ > 120^\circ$) occurred most frequently in the TR subgroup with AF (20.0% [16/80] vs 0% [0/50] vs 8.6% [9/105], $P < .001$; Figure 3B). Furthermore, in the AF group, patients with severe TR ($n = 30$) had a more posteriorly displaced TA than those with moderate TR ($98.9^\circ \pm 36.5^\circ$ vs $81.9^\circ \pm 34.6^\circ$; $P = .04$).

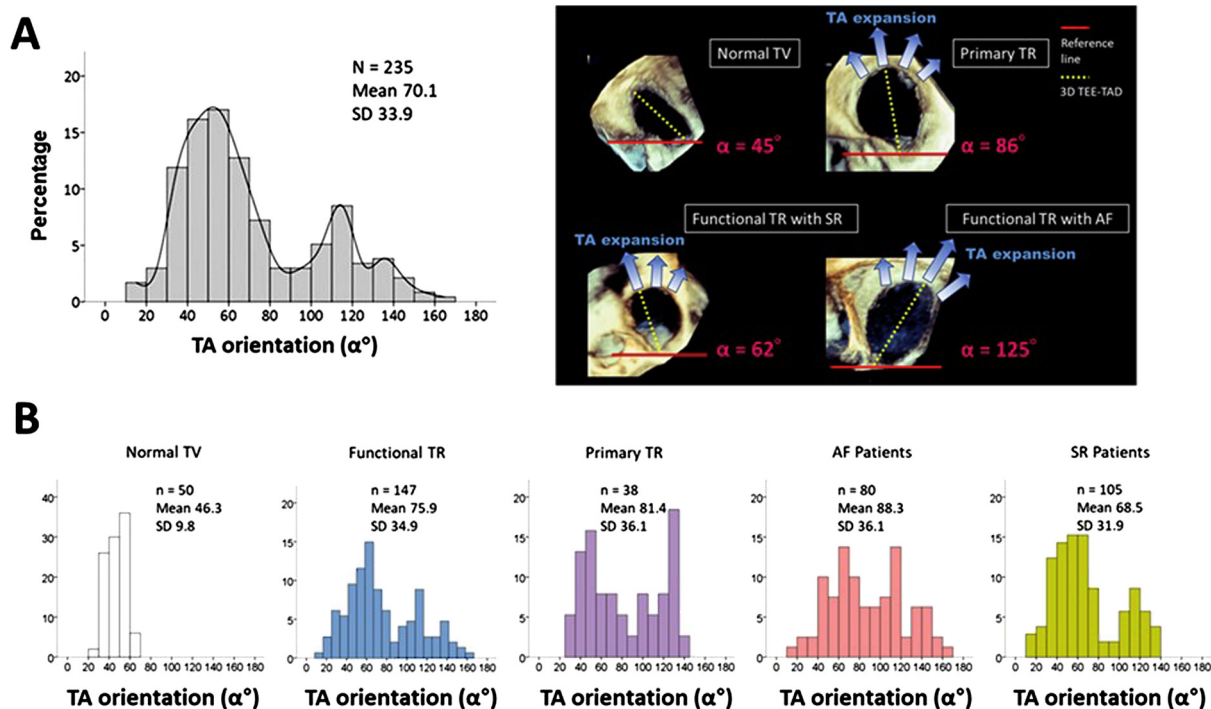


Figure 3 Distribution of TA orientation. **(A)** Total patient population and **(B)** according to TR subgroups. Note the two most frequent orientations in these histograms and examples of TA orientations, with the posteriorly displaced TA most frequently noted in patients with AF.

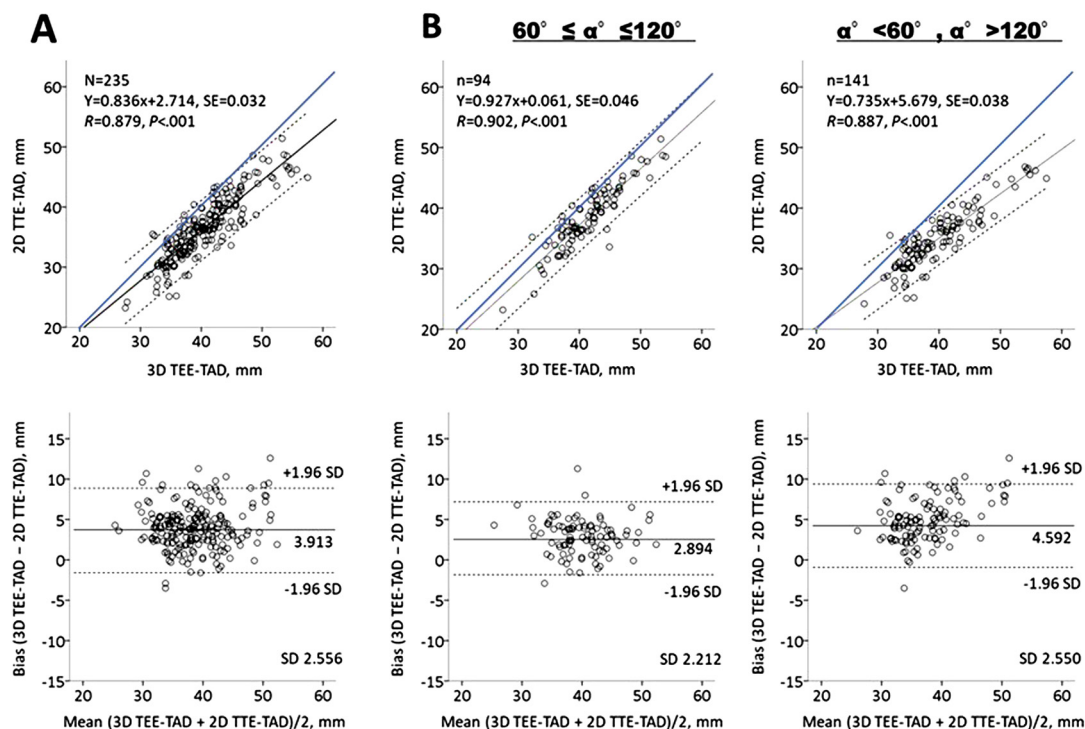


Figure 4 Correlation and agreement between 3D TEE-TAD and 2D TTE-TAD. **(A)** Total patient population. **(B)** Stratified by tricuspid annular orientation. The upper panels show scatterplots of the correlation between 3D TEE-TAD and 2D TTE-TAD with a regression line (solid lines) and 95% CI (dotted lines) and with a line of identity (blue line). The lower panels depict the Bland-Altman plots with the mean bias (solid lines) and 95% limits of agreement (dotted lines).

Table 3 Factors related to the bias between 3D TEE-TAD and 2D TTE-TAD in patients with TR ($N = 185$)

	Univariable	Multivariable ^{*,†}			
	<i>P</i>	Coefficient (95% CI)	<i>t</i>	<i>P</i>	VIF
3D TEE-TAD	<.001	0.183 (0.100-0.266)	4.345	<.001	1.955
TA eccentricity index	.55	-3.358 (-9.320-2.604)	-1.112	.27	1.183
Absolute value of $90^\circ - \alpha^\circ$	<.001	0.071 (0.052-0.091)	7.257	<.001	1.048

VIF, Variance inflation factor.

*All variables were adjusted for age, sex, body surface area, AF, and average vena contracta width.

† $R^2 = 0.372$.

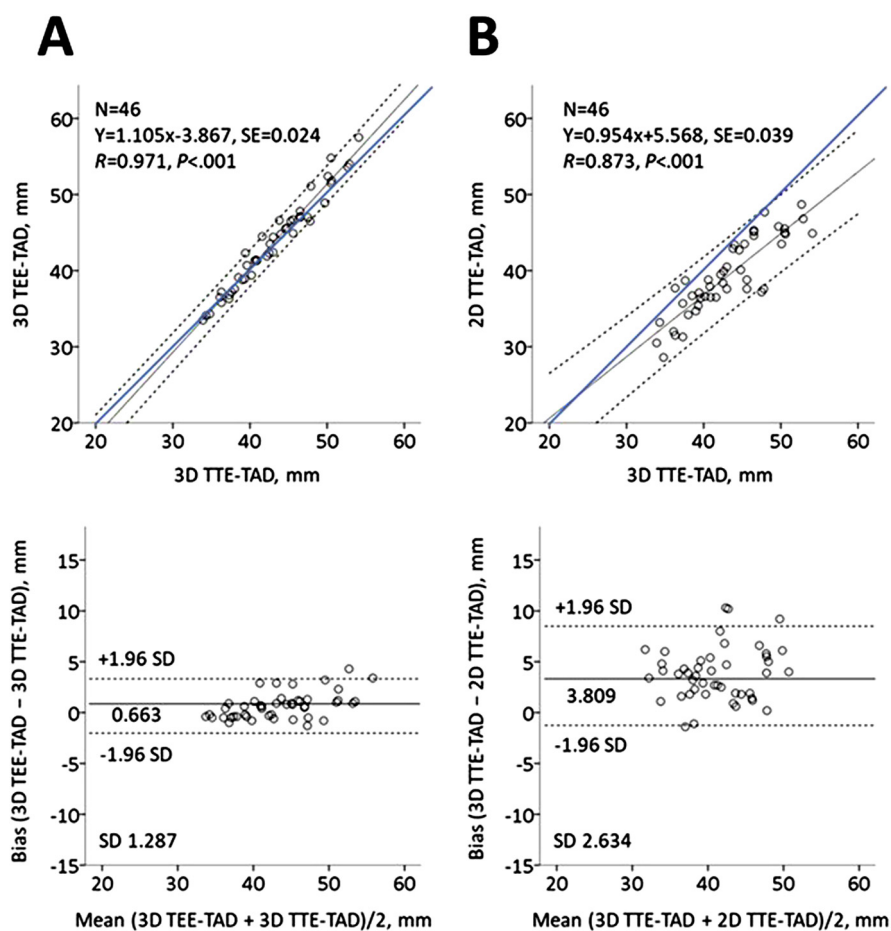


Figure 5 Substudy results: correlation and agreement of 3D TTE-TAD with 3D TEE-TAD (**A**) and 2D TTE-TAD (**B**). The upper panels show scatterplots of the correlation of 3D TTE-TAD with 3D TEE-TAD and 2D TTE-TAD with a regression line (solid lines) and 95% CI (dotted lines) and with a line of identity (blue line). The lower panels depict the Bland-Altman plots with the mean bias (solid lines) and 95% limits of agreement (dotted lines).

Correlation and Agreement between 3D TEE-TAD and 2D TTE-TAD

In the total patient population, an excellent correlation was found between 3D TEE-TAD and 2D TTE-TAD ($R = 0.879$, $P < .001$; Figure 4A), but 2D TTE-TAD was significantly smaller than 3D TEE-TAD (35.9 ± 5.4 vs 39.8 ± 5.7 mm; $P < .001$; bias, 3.9 ± 2.6 mm; limits of agreement, -1.1 - 8.9 mm). We divided the patient population into two subsets according to the value of α° ($60^\circ \leq \alpha^\circ \leq 120^\circ$ vs $\alpha^\circ < 60^\circ$ or $\alpha^\circ > 120^\circ$). TA orientation did

not affect the excellent correlation; however, more prominent bias between 3D TEE-TAD and 2D TTE-TAD was observed in the subset of patients with $\alpha^\circ < 60^\circ$ or $\alpha^\circ > 120^\circ$ (bias, 4.6 ± 2.6 mm; limits of agreement, -0.4 - 9.6 mm; Figure 4B).

Determinants of the Bias between 3D TEE-TAD and 2D TTE-TAD

To explore factors related to the bias between 3D TEE-TAD and 2D TTE-TAD in patients with TR ($n = 185$), multivariable linear regression

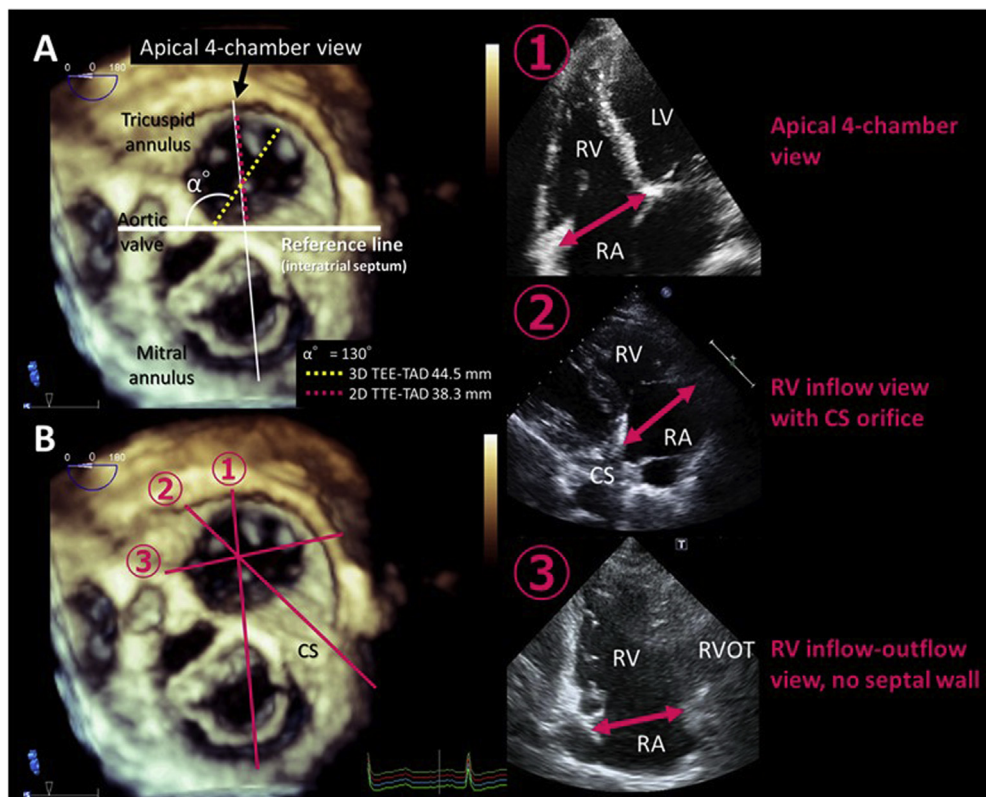


Figure 6 The angle difference between major TA axis and various 2D TTE planes. **(A)** A representative case with large absolute value of $90^\circ - \alpha^\circ$ and posteriorly displaced TA presenting a large bias of 6.2 mm between 3D TEE-TAD and 2D TTE-TAD. The solid white line represents the reference line parallel to the interatrial septum. **(B)** Orientations of various 2D TTE planes for the measurement of TAD including the apical four-chamber view, RV inflow view with CS orifice, and RV inflow-outflow view approximately parallel to the coronal section of the RV. It can be seen that none of these three 2D image planes captures the largest TAD. CS, Coronary sinus; LV, left ventricle; RA, right atrium; RVOT, RV outflow tract.

was performed with the following covariates: 3D TEE-TAD, TA eccentricity index, and the absolute value of $90^\circ - \alpha^\circ$. After adjustment for TR severity and several demographic variables including age, sex, body surface area, and AF, a larger 3D TEE-TAD (coefficient, 0.183; 95% CI, 0.100-0.266) and larger absolute value of $90^\circ - \alpha^\circ$ (coefficient, 0.071; 95% CI, 0.052-0.091) remained as independent determinants of the bias between 3D TEE-TAD and 2D TTE-TAD (Table 3). Namely, when the direction of TA expansion deviates from 90° , the largest dimension is missed in an apical four-chamber view on 2D TTE.

Substudy Results: Correlation and Agreement of 3D TTE-TAD with 3D TEE-TAD and 2D TTE-TAD

The correlation between 3D TTE-TAD and 3D TEE-TAD was excellent ($R = 0.971$, $P < .001$) with a slight underestimation of 3D TTE-TAD ($P = .03$; bias, 0.6 ± 1.3 mm; Figure 5A). In addition, an excellent correlation was also found between 3D TTE-TAD and 2D TTE-TAD ($R = 0.873$, $P < .001$), but 2D TTE-TAD was significantly smaller than 3D TTE-TAD ($P < .001$; bias, 3.8 ± 2.6 mm; Figure 5B).

Reproducibility

Intraobserver and interobserver variability in the 3D measurements was as follows: 3D TEE-TAD, 0.8 ± 0.7 mm and 1.3 ± 1.1 mm; TA eccentricity index, 0.03 ± 0.03 and 0.05 ± 0.03 ; and α° , $3.4^\circ \pm 3.0^\circ$ and $5.1^\circ \pm 3.9^\circ$, respectively. Intraclass correlations (95% CI) for each of the mea-

surements were as follows: 3D TEE-TAD, 0.94 (0.92-0.96) and 0.93 (0.91-0.95); TA eccentricity index, 0.93 (0.91-0.95) and 0.93 (0.90-0.95); and α° , 0.92 (0.89-0.94) and 0.89 (0.85-0.93), respectively.

DISCUSSION

The present study substantiates the hypotheses suggested by several prior studies, highlighting the putative value of a 3D echocardiography-based evaluation of the TA for the measurement of TAD.^{9,14} Three-dimensional TEE can assess TA orientation reproducibly and precisely in multiplanar reconstruction of the TV using guidance on the corresponding 3D volume rendering. Its main findings in this cohort of patients with grade $\geq 3+$ TR are the following: (1) compared with normal controls, TA size, shape, and orientation were altered in patients with TR, showing a more dilated, circular, and posteriorly displaced TA; (2) AF rhythm, rather than TR etiology, may be associated with more posterior TA expansion; (3) despite an excellent correlation between 3D TEE-TAD and 2D TTE-TAD, 2D TTE-TAD was significantly smaller than 3D TEE-TAD; and (4) not only TA size but also its orientation were multivariable determinants of the underestimation of 2D TTE-TAD.

Figure 6 depicts the angle difference between major TA axis and various 2D TTE planes. The angle between the 2D TTE apical four-chamber view and interatrial septum parallel to the vertical axis is usually closer to 90° . Therefore, the absolute value of $90^\circ - \alpha^\circ$ is thought

to be approximately the angle difference between the direction of the 2D TTE apical four-chamber view and the direction of TA expansion (Figure 6A), which was independently associated with the bias between 3D TEE-TAD and 2D TTE-TAD in our regression model.

Tricuspid Annular Dilatation in Patients with TR

Despite the association of significant TR with increased mortality,² the disease often remains untreated partially because TR itself has not been comprehensively and extensively studied. Thus far, the TV deformations including annular dilatation, leaflet tethering, and insufficient coaptation status have been shown to be the main mechanisms in the development of functional TR.^{6,10,15} As first reported by Sagie *et al.*,¹⁶ TA dilatation is the most consistent and important determinant of significant TR. Kim *et al.*¹⁷ evaluated 64 patients with TR and RV dilatation and found that 2D TTE-TAD showed the independent associations with TR effective regurgitant orifice area. Utsunomiya *et al.*¹⁰ reported 36 patients with TR and RA dilatation secondary to long-standing AF, all of whom had a more dilated, circular, and dysfunctional TA compared with normal controls. They also showed the 3D TEE-derived TA area was a multivariable determinant of TR vena contracta width irrespective of TR etiologies.¹⁰ On the other hand, the present study focused not only on the size and shape of the dilated TA but also on its orientation. The TA orientation, which represents the direction of TA expansion, was altered in patients with TR compared with normal controls; however, its distribution ranged widely, suggesting the clinical importance of asymmetrical TA expansion.

Using 3D echocardiography-based TV screening, we can determine TR subgroups stratified by TR etiology and functional and primary TR. However, we did not find fundamental differences in TA area, shape, and orientation according to TR etiology. The posteriorly displaced TA was frequently noted in patients with AF. This posterior TA expansion might be explained by the fact that the posterior wall is the only region of the TA that is not constrained by other cardiac structures and thus there is less support in this region. In the present study, a modest correlation between TA orientation and RA/RV end-systolic volume ratio was observed in the TR subgroup with AF ($R = 0.529$, $P < .001$; Supplemental Figure 1). However, the probable interaction between right heart remodeling and the changes in TA morphology remains unclear.

Effects of TA Orientation on the TAD Measurement

Tricuspid annular dilatation appears earlier in the course of the disease.¹⁸ Thus, current recommendations have incorporated enlarged TAD in addition to TR severity as an indication for concomitant TV annuloplasty at the time of left-sided heart surgery to avoid the occurrence of significant late TR and to promote RV reverse remodeling and improvement of RV function.⁵ In daily clinical practice, 2D TTE is the most common modality used to measure TAD. Standard views of the TV on 2D TTE include the RV inflow, parasternal short-axis, and apical four-chamber views, and recently the RV-focused view has also been recommended as a potentially useful imaging window from which to visualize the TV.^{4,11} However, a 2D TTE measurement of the maximum dimension of the TV annulus will not be as accurate as a 3D echocardiographic measurement since the TV annulus is not optimally oriented for it to be measured from an apical four-chamber view.¹⁹

During the past decade, 3D echocardiography has been developed, which allows accurate quantitative and qualitative analysis of cardiac structures including the TV.^{7-10,15} Dreyfus *et al.*⁹ evaluated 194 patients with wide range of TR severity and compared 2D TTE-TAD

measured in an apical four-chamber view and 3D TEE-TAD defined as the longest dimension of the TA, showing the 2D TTE-TAD as being smaller than the 3D TEE-TAD with a systematic 4 mm underestimation. Addetia *et al.*¹⁴ analyzed 2D TTE and 3D TEE in 209 healthy volunteers and found that the longest 3D TA dimension was significantly larger than diameters measured from both 2D TTE and 3D multiplanar reconstruction. Similar to the results of Dreyfus *et al.*⁹ and Addetia *et al.*,¹⁴ we also found in patients with TR that 2D TTE-TAD is highly correlated with 3D TEE-TAD but 2D TTE-TAD is significantly smaller than 3D TEE-TAD, with a mean bias of 3.9 ± 2.6 mm.

A very important point from our study is that when TA orientation deviates from 90°, the largest dimension is missed in an apical four-chamber view on 2D TTE (Figure 6A). Theoretically, in such cases, other 2D TTE planes including the RV inflow view with coronary sinus orifice and the RV inflow-outflow view approximately parallel to the coronal section of the RV would be more accurate to identify the largest TA dimension than the apical four-chamber view (Figure 6B).

Clinical Implications

Ring annuloplasty is currently considered as the standard surgical procedure for TR; therefore, there is a primary emphasis on TA size in the current guidelines. In contrast, TA orientation has received less attention than TA size, and our findings indicate that TA orientation differs among normal controls and TR subgroups. As for the transcatheter TV leaflet clip procedure, a recent study showed that a central/antero-septal TR jet location and small coaptation gap size independently predicted procedural success.²⁰ Therefore, assessing the orientation of the dilated annulus, detecting the exact location of proximal flow convergence, and then first trying to capture the diseased lesion correctly might be of vital importance for this procedure. With anticipation of improvements in transcatheter TV interventions in the future, this 3D echocardiography information may be utilized to improve the chances for procedural success.

Limitations

This study has several limitations. First, this was a retrospective single-center study from a tertiary referral center. Therefore, this study is not free of referral bias. Second, our results may not guarantee an excellent feasibility for measuring 3D TV parameters in general. To obtain clear 3D TEE images that make accurate TV measurements possible, it is of great importance to improve 3D images of the TV leaflets with slight and proper modification of gain setting, probe depth, angle, focus distance, and size of area of interest and to ensure enough frame rate. In addition, 3D TEE is not the only tool available to accurately obtain TAD. A recent publication by Volpato *et al.*²¹ reported the usefulness of 3D TTE-based TAD measurement in 70 patients with various cardiac conditions including significant TR (~20% of study population). Also, in the present study, a very small bias between 3D TTE-TAD and 3D TEE-TAD was observed in patients with grade $\geq 3+$ TR (Figure 5A). Third, our study is limited by the lack of gold standard cardiac computed tomography imaging or pathologic confirmation. Most recently, Praz *et al.*²² investigated 38 patients with severe TR and showed that semiautomated indirect planimetry results in high agreement between TEE and computed tomography for TA area and perimeter. Also, in the present study, the mitral module of the QLAB MVN software was used in an off-label fashion for semiautomated indirect measurement of 3D TEE-TAD during diastole. However, the accuracy of 3D TEE-TAD and TA orientation needs to be validated. Fourth, while the AF group does have more patients with TA orientation $>120^\circ$, it is also important to note that the large

majority of AF patients have TA orientation $<120^\circ$ (Figure 3B). Therefore, clinical factors associated with the occurrence of more posteriorly displaced TA in AF patients, such as AF duration, should be elucidated. Finally, serial TV assessment and clinical follow-up were not performed; therefore, the actual impact of TA orientation on worsening TR and clinical outcomes remains unclear.

CONCLUSION

The inconsistencies between measured 2D TTE-TAD and the actual annular diameter can be explained through morphologic factors such as TA size and orientation. In patients with clinically significant TR, a 3D cutoff value for TA enlargement and a comprehensive method for the measurement of TAD using both 2D and 3D echocardiography need to be established.

ACKNOWLEDGMENTS

We thank Nobuo Ninomiya, Hiroshi Ofuji, and Takayuki Hataoka, from Philips Electronics Japan, for their technical assistance.

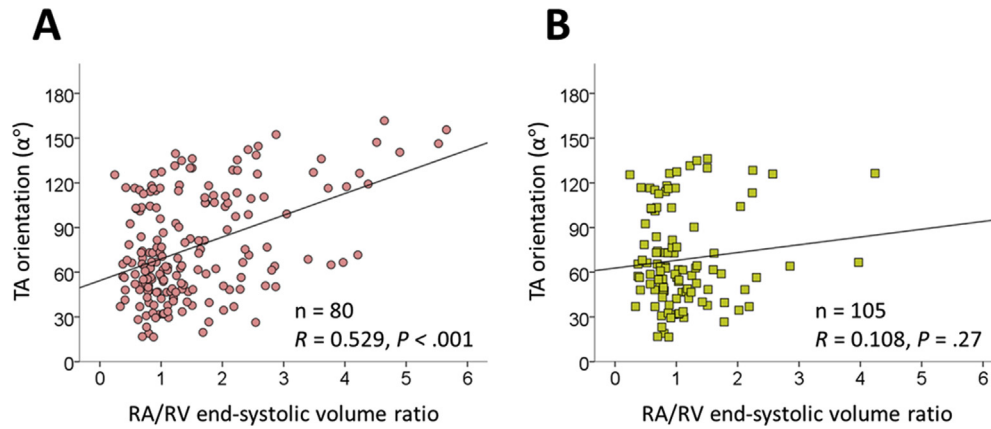
SUPPLEMENTARY DATA

Supplementary data to this article can be found online at <https://doi.org/10.1016/j.echo.2019.09.016>.

REFERENCES

1. Thomas KL, Jackson LR 2nd, Shrader P, Ansell J, Fonarow GC, Gersh B, et al. Prevalence, characteristics, and outcomes of valvular heart disease in patients with atrial fibrillation: insights from the ORBIT-AF (Outcomes Registry for Better Informed Treatment for Atrial Fibrillation). *J Am Heart Assoc* 2017;6:e006475.
2. Nath J, Foster E, Heidenreich PA. Impact of tricuspid regurgitation on long-term survival. *J Am Coll Cardiol* 2004;43:405-9.
3. Chikwe J, Itagaki S, Anyanwu A, Adams DH. Impact of concomitant tricuspid annuloplasty on tricuspid regurgitation, right ventricular function, and pulmonary artery hypertension after repair of mitral valve prolapse. *J Am Coll Cardiol* 2015;65:1931-8.
4. Rudski LG, Lai WW, Afilalo J, Hua L, Handschumacher MD, Chandrasekaran K, et al. Guidelines for the echocardiographic assessment of the right heart in adults: a report from the American Society of Echocardiography endorsed by the European Association of Echocardiography, a registered branch of the European Society of Cardiology, and the Canadian Society of Echocardiography. *J Am Soc Echocardiogr* 2010;23:685-713.
5. Nishimura RA, Otto CM, Bonow RO, Carabello BA, Erwin JP 3rd, Fleisher LA, et al. 2017 AHA/ACC focused update of the 2014 AHA/ACC guideline for the management of patients with valvular heart disease: a report of the American College of Cardiology/American Heart Association Task Force on Clinical Practice Guidelines. *Circulation* 2017;135:e1159-95.
6. Ton-Nu TT, Levine RA, Handschumacher MD, Dorer DJ, Yosefy C, Fan D, et al. Geometric determinants of functional tricuspid regurgitation: insights from 3-dimensional echocardiography. *Circulation* 2006;114:143-9.
7. Stankovic I, Daraban AM, Jasaityte R, Neskovic AN, Claus P, Voigt JU. Incremental value of the en face view of the tricuspid valve by two-dimensional and three-dimensional echocardiography for accurate identification of tricuspid valve leaflets. *J Am Soc Echocardiogr* 2014;27:376-84.
8. Addetia K, Yamat M, Mediratta A, Medvedofsky D, Patel M, Ferrara P, et al. Comprehensive two-dimensional interrogation of the tricuspid valve using knowledge derived from three-dimensional echocardiography. *J Am Soc Echocardiogr* 2016;29:74-82.
9. Dreyfus J, Durand-Viel G, Raffoul R, Alkhoder S, Hvass U, Radu C, et al. Comparison of 2-dimensional, 3-dimensional, and surgical measurements of the tricuspid annulus size: clinical implications. *Circ Cardiovasc Imaging* 2015;8:e003241.
10. Utsunomiya H, Itabashi Y, Mihara H, Berdejo J, Kobayashi S, Siegel RJ, et al. Functional tricuspid regurgitation caused by chronic atrial fibrillation: a real-time 3-dimensional transesophageal echocardiography study. *Circ Cardiovasc Imaging* 2017;10:e004897.
11. Zoghbi WA, Adams D, Bonow RO, Enriquez-Sarano M, Foster E, Grayburn PA, et al. Recommendations for noninvasive evaluation of native valvular regurgitation: a report from the American Society of Echocardiography Developed in collaboration with the Society for Cardiovascular Magnetic Resonance. *J Am Soc Echocardiogr* 2017;30:303-71.
12. Song JM, Jang MK, Choi YS, Kim YJ, Min SY, Kim DH, et al. The vena contracta in functional tricuspid regurgitation: a real-time three-dimensional color Doppler echocardiography study. *J Am Soc Echocardiogr* 2011;24:663-70.
13. Lang RM, Badano LP, Tsang W, Adams DH, Agricola E, Buck T, et al. EAE/ASE recommendations for image acquisition and display using three-dimensional echocardiography. *J Am Soc Echocardiogr* 2012;25:3-46.
14. Addetia K, Muraru D, Veronesi F, Jenei C, Cavalli G, Besser SA, et al. 3-dimensional echocardiographic analysis of the tricuspid annulus provides new insights into tricuspid valve geometry and dynamics. *JACC Cardiovasc Imaging* 2019;12:401-12.
15. Afilalo J, Grapsa J, Nihoyannopoulos P, Beaudoin J, Gibbs JS, Channick RN, et al. Leaflet area as a determinant of tricuspid regurgitation severity in patients with pulmonary hypertension. *Circ Cardiovasc Imaging* 2015;8:e002714.
16. Sagie A, Schwammenthal E, Padiol LR, Vazquez de Prada JA, Weyman AE, Levine RA. Determinants of functional tricuspid regurgitation in incomplete tricuspid valve closure: Doppler color flow study of 109 patients. *J Am Coll Cardiol* 1994;24:446-53.
17. Kim HK, Kim YJ, Park JS, Kim KH, Kim KB, Ahn H, et al. Determinants of the severity of functional tricuspid regurgitation. *Am J Cardiol* 2006;98:236-42.
18. Shiran A, Sagie A. Tricuspid regurgitation in mitral valve disease incidence, prognostic implications, mechanism, and management. *J Am Coll Cardiol* 2009;53:401-8.
19. Miglioranza MH, Mihaila S, Muraru D, Cucchini U, Iliceto S, Badano LP. Dynamic changes in tricuspid annular diameter measurement in relation to the echocardiographic view and timing during the cardiac cycle. *J Am Soc Echocardiogr* 2015;28:226-35.
20. Besler C, Orban M, Rommel KP, Braun D, Patel M, Hagl C, et al. Predictors of procedural and clinical outcomes in patients with symptomatic tricuspid regurgitation undergoing transcatheter edge-to-edge repair. *JACC Cardiovasc Interv* 2018;11:1119-28.
21. Volpato V, Lang RM, Yamat M, Veronesi F, Weinert L, Tamborini G, et al. Echocardiographic assessment of the tricuspid annulus: the effects of the third dimension and measurement methodology. *J Am Soc Echocardiogr* 2019;32:238-47.
22. Praz F, Khalique OK, Dos Reis Macedo LG, Pulerwitz TC, Jantz J, Wu IY, et al. Comparison between three-dimensional echocardiography and computed tomography for comprehensive tricuspid annulus and valve assessment in severe tricuspid regurgitation: implications for tricuspid regurgitation grading and transcatheter therapies. *J Am Soc Echocardiogr* 2018;31:1190-202.e3.

SUPPLEMENTARY DATA



Supplemental Figure 1 Correlations between TA orientation (α°) and RA/RV end-systolic volume ratio. **(A)** Patients with AF. **(B)** Patients with SR.